Individually Ventilated Cages Impose Cold Stress on Laboratory Mice: A Source of Systemic Experimental Variability

John M David,[1,*] Scott Knowles,[1] Donald M Lamkin,[2] and David B Stout[1]

Individual ventilated cages (IVC) are increasing in popularity. Although mice avoid IVC in preference testing, they show no aversion when provided additional nesting material or the cage is not ventilated. Given the high ventilation rate in IVC, we developed 3 hypotheses: that mice housed in IVC experience more cold stress than do mice housed in static cages; that IVC-induced cold stress affects the results of experiments using mice; and that, when provided shelters, mice behaviorally thermoregulate and thereby rescue the cold-stress effects of IVC. To test these hypotheses, we housed mice in IVC, IVC with shelters, and static cages maintained at 20 to 21 °C. We quantified the cold stress of each housing system on mice by assessing nonshivering thermogenesis and brown adipose vacuolation. To test housing effects in a common, murine model of human disease, we implanted mice with subcutaneous epidermoid carcinoma cells and quantified tumor growth, tumor metabolism, and adrenal weight. Mice housed in IVC had histologic signs of cold stress and significantly higher nonshivering thermogenesis, smaller subcutaneous tumors, lower tumor metabolism, and larger adrenal weights than did mice in static cages. Shelters rescued IVC-induced nonshivering thermogenesis, adrenal enlargement, and phenotype-dependent cold-mediated histologic changes in brown adipose tissue and tumor size. IVC impose chronic cold stress on mice, alter experimental results, and are a source of systemic confounders throughout rodent-dependent research. Allowing mice to exhibit behavioral thermoregulation through seeking shelter markedly rescues the experiment-altering effects of housing-imposed cold stress, improves physiologic uniformity, and increases experimental reproducibility across housing systems.

Abbreviations: BAT, brown adipose tissue; ^{18}F-FDG, fluorodeoxyglucose; MARS, Mouse Atlas Registration system; IVC, individually ventilated cage; PET, positron emission tomography; ROI, region of interest; SUV, standard uptake value.

Individual ventilated cages (IVC) have been increasing in popularity because they accommodate increased stocking density and reduce the spread of murine infectious pathogens, allergens, and biohazardous agents.[7] Despite limited research examining the welfare of mice housed in IVC has been published, we know that mice housed in IVC exhibit enhanced anxiety, reduced general activity, and increased startle response.[23,27] In preference testing, mice avoid IVC but show no preference when supplied additional nesting material or when the air supply is covered,[1] hinting that the ventilation of IVC may impose cold stress in mice. In light of the high rate of ventilation within IVC, ranging from 40 to 80 cage changes hourly,[1] our group developed 3 hypotheses: that mice housed in IVC experience significantly more cold stress than do mice housed in static cages; that the additional cold stress imposed by IVC affects the results of experiments using mice to model human disease; and that, when provided shelters, mice behaviorally thermoregulate and thereby rescue the effects of IVC-induced cold stress.

The first and preferred cold-adaptive thermoregulatory response of rodents is behavioral, such as building nests and seeking shelters.[12] Behavioral responses are crucial to the survival of mice, whose large surface-area–to–volume ratio makes them especially prone to cold stress.[17] The routine barren shoebox-type cages used in laboratory settings limit murine thermoregulatory behavior.[12,17]

If behavioral adaptations are overwhelmed, rodents experience a net loss of heat to the environment, and compensatory thermogenesis mechanisms are activated.[17] The primary compensatory physiologic reaction in rodents is nonshivering thermogenesis, which is mediated through brown adipose tissue (BAT).[2,3] BAT is a cold-responsive tissue derived from myoblasts, sharing similar embryologic origins with muscle,[33] and is rich in mitochondria capable of high oxidative metabolism.[17,28] The largest deposit of BAT in rodents is located in the interscapular region and smaller deposits are adjacent to sympathetic ganglions and the adrenal glands, highlighting close ties with the sympathetic nervous system.[29] Indeed, BAT cells have high expression of β_3-adrenergic receptors and are activated by catecholamines that are produced by resident macrophages and by hypothalamus-mediated sympathetic trunk activity.[4,29,30] When active, BAT receives a large proportion of cardiac outflow and oxidizes glucose, producing heat and thereby maintaining core body temperature.[9] BAT thermoregulatory functions are crucial to maintaining the body temperature of small mammals and allows rodents to adapt to a wide range of climates.[2]

However, nonshivering thermogenesis has high energy costs[4] and can alter a variety of homeostasis parameters, including increasing basal metabolism[6,8] and sympathetic tone.[29] The high energy demands of chronic cold-stress have significant scientific impacts on a variety of murine models.[26] There are several known examples: mice housed at routine vivarium temperatures have a blunted febrile (immunosuppression) response to the potent

pyrogen LPS but, when housed at thermoneutral temperatures, have febrile patterns similar to those of humans;[32] mice have higher mean atrial pressure and heart rate at routine vivarium temperatures compared with thermoneutral temperatures;[35] and an obesogenic knockout mouse only develops obesity at thermoneutral temperatures.[7] Cold stress has the potential to affect almost every field of murine-dependent science and can alter research results, sometimes in unpredictable ways.[26]

Concerned with the potential effects of housing-dependent cold stress on scientific outcomes, we designed the following experiment to measure housing effects and behavioral thermoregulation on physiology and experimental outcomes. We quantitated cold stress by measuring BAT activity by using thermography, histology, and positron emission tomography (PET). We choose thermography and PET to assay BAT activity because—unlike classic metrics such as bomb calorimetry—they allow us to quantify cold stress in the vivarium without disrupting housing conditions.[18] Subcutaneous tumors are an ideal model in which to test potential cold-related effects because this model is extremely common (and therefore important to many investigators) and its metabolism is sensitive to environmental temperatures.[10]

Materials and Methods

Animals. Male CB17/lcr-*Prkdc^scid^/lcrlcoCrl* (*Prdkc^scid^*) and Crl: Nu-*Foxn1*^Nu^ (Nu-*Foxn1*^Nu^) mice (age, 10 wk) were acquired from Charles River Laboratories and housed in an AAALAC-accredited facility. This study used a total of 24 mice equally divided between Prdkc^scid^ and Nu-*Foxn1*^Nu^ mice, which are deficient in lymphocytes and thus support the growth of human subcutaneous tumors. In addition, Nu-*Foxn1*^Nu^ mice experience greater cold stress than do hirsute mice[6] and represent an extreme, but common, hairless phenotype of laboratory mice. SPF status was monitored quarterly by dirty-bedding sentinels screened for mouse parvovirus, minute virus of mice, mouse norovirus, mouse hepatitis virus, Sendai virus, lymphocytic choriomeningitis virus, polyomavirus, K virus, pneumonia virus of mice, mouse adenovirus, epizootic diarrhea of infant mice (rotavirus), mouse encephalomyelitis virus, reovirus, ectromelia virus, *Mycoplasma pulmonis*, and endo- and ectoparasites. All mice were fed a commercial diet (NIH31, Harlan Teklad, Madison, WI) and received HCl-acidified, reverse-osmosis–purified water ad libitum. The room was maintained at a temperature of 20 to 21 °C, relative humidity of 30% to 70%, 10 to 15 room air changes hourly, and had a 12:12-h photoperiod. All experiments were approved by the IACUC of the University of California, Los Angeles.

Study design. All mice were singly housed to control for social huddling in 1 of 3 environments: an IVC (InnoRack, InnoVive, San Diego, CA), an IVC with a red translucent igloo-shaped shelter (InnoDome, InnoVive), or a static cage (InnoVive; *n* = 4 per group in a balanced 2 × 3 factorial design). The IVC were ventilated at 60 air changes hourly (negative pressure). Each cage contained 200 g of corncob bedding (InnoVive). Cages were changed every 7 d.

The mice were allowed to acclimate to the new environment for 72 h. Nonshivering thermogenesis was measured by thermography for 7 d. Then, the mice were implanted subcutaneously with epidermal carcinoma tumor cells (A431), which were allowed to grow for 14 d prior to PET imaging. At the end of the study, the mice were euthanized for tissue harvest.

Thermography. To measure cold stress in the mice in each housing group, we quantified nonshivering thermogenesis of BAT by using infrared thermography according to a previously

established protocol.[6] Briefly, each cage was removed from the rack and placed into a hood, and each mouse was imaged by using a tripod-mounted thermography camera (model T420, FLIR, Nashua, NH) at 0.6 m. Sampling occurred between 0900 and 1000 each day to minimize circadian rhythm effects,[38] and the entire process approximately 20 s per mouse and did not require handling. Short sampling time is necessary to minimize artificial activation of BAT, which can occur within a few moments.

A line profile measuring radiated heat was drawn over the BAT region, and an internal control line profile was drawn over the most caudal rib (QuickReport version 1.2, FLIR). Emissivity was set to 0.94 for *Prdkc^scid^* mouse fur and to 0.98 for the skin of NU-*Foxn1*^nu^ mice.[14] ΔT BAT, a measure of nonshivering thermogenesis, was calculated by subtracting the average temperature of the control region of interest ($ROI_{control}$) from the average temperature of the ROI_{BAT}.[6]

Subcutaneous tumor model. The human epidermoid carcinoma cell line A431 was grown under routine, sterile conditions in DMEM supplemented with 10% FBS;[15] the cells were kindly provided by the Dr Shuang Hou (Crump Institute for Molecular Imaging, Los Angeles, CA). Cell viability was confirmed prior to implantation (Vi-Cell Viability Counter, Beckman Coulter, Brea, CA). After 7 d of thermography sampling, the mice were anesthetized with 2% isoflurane and subcutaneously implanted with 1×10^6 A431 cells suspended in 50% PBS, 50% Matrigel (Fisher Scientific, Pittsburgh, PA) according to a previously established protocol.[10] The tumors were allowed to grow for 14 d before PET imaging.

PET. At 14 d after implantation, mice were injected intraperitoneally with approximately 35 µCi of the glucose analog ^18^F-fluorodeoxyglucose (^18^F-FDG) to quantify the uptake of glucose and then returned to their home cage on their respective ventilated or static racks. During the uptake phase, ^18^F-FDG is taken up through glucose transporters and enzymatically phosphorylated by hexokinase; the phosphorated form cannot be metabolized and becomes trapped within glycolytic cells. The accumulation of ^18^F-FDG within metabolically activate cells is therefore an indication of glucose utilization. After a routine 50-min uptake period in conscious mice, mice were anesthetized before imaging by using 2% isoflurane (Phoenix, St Joseph, MO) mixed with 100% oxygen and placed in heated imaging chambers (Sofie Bioscience, Culver City, CA). PET imaging, a 2D X-ray radiograph, and a lateral photograph were acquired by using a preclinical PET imaging system (Genisys4, Sofie Biosciences).

As an anatomic compliment to the PET scan, a microCT scan was performed on each mouse (microCAT II, Siemens Preclinical Solutions, Knoxville, TN). The exposure settings were 70 kVp, 500 mAs, 500 ms at 360° rotation in 1° steps with a 2-mm aluminum filtration. CT was reconstructed by using a modified Feldkamp process developed by Dr Richard Taschereau (University of California, Los Angeles).

PET images were generated by using a maximum likelihood expectation maximization algorithm,[24] reconstructed with 60 iterations, normalized for detector response, and corrected for isotope decay and photon attenuation. Mouse Atlas Registration System (MARS) software[39,40] used the single-projection radiograph and the lateral photograph to generate an atlas of mouse organ locations and a coregistered standardized ROI placement.[39,40] Images reconstructed to produce a fused PET–CT image, providing both metabolic and anatomic information.

The PET images of BAT ^{18}F-FDG uptake were analyzed (A Medical Image Data Examiner, version 1.0.1, Andy Leoning, http://sourceforge.net/projects/amide/), and ROI$_{BAT}$ was drawn by using MARS automation software.[39,40] Because BAT is a 'dark organ' that is undistinguishable from surrounding white fat by using current anatomic imaging techniques, we used MARS to standardize ROI placement and minimize subjectivity of location and quantification of BAT ^{18}F-FDG uptake. Tissue density was assumed to be 1 g/mL. All radioactivity values were corrected for attenuation and decay. The BAT standard uptake value (SUV) was calculated according to the following formula:

$$SUV_{BAT} = ROI_{BAT} \text{ (Bq÷ mL)} ÷ [\text{injected dose (Bq)} × \text{body weight (g)}].$$

Tumor ^{18}F-FDG uptake was quantified by drawing a 2-mm spherical ROI at the center of the tumor located by CT. Tumor SUV was calculated by using the same formula as SUV$_{BAT}$.

Histology. On histology, BAT cell cytoplasm from a warm-adapted mouse is dominated by monolobular lipid droplets and appears morphologically similar to white adipose.[25] Conversely, BAT cells from cold-adapted mice are foamy and finely vacuolated.[25] To quantitate BAT cold-adaption, mice were euthanized, and BAT, adrenals, and tumors were harvested, weighed (model M120, Denver Instrument, Bohemia, NY), fixed in 4% formalin, sectioned, and stained with hematoxylin and eosin. This method was used rather than assessing fat-stained frozen tissue sections, which are prone to morphologic distortions, limiting their quantitative value.[34]

BAT histology was viewed by using a light microscope (BX41, Olympus, Center Valley, PA) and photographed with a digital camera (DP25, Olympus) at 40× magnification. To minimize sampling bias and anomalous sectioning skewing results, a blinded observer digitally photographed 3 representative high-power-field samples of BAT from each animal. Non-BAT tissues, primarily small blood vessels, were cropped from the field of view prior to image processing (Wright Cell Imaging Facility modification of ImageJ, version 1.37c, Wayne Rasband, NIH, http://www.uhnresearch.ca). The images were separated into red, green, and blue channels by using the color deconvolution plugin. To quantitate vacuole size, the green channel was converted to a binary image by using the threshold tool, eroded, dilated with a macro to separate the converging vacuoles, and quantified with the particle analysis tool.

Statistical analysis. ΔT BAT and BAT vacuole size were tested for significant differences and interactions by using repeated-measures ANOVA to account for multiple sampling from each mouse. Housing group and phenotype (*Prdkc^{scid}* or NU-*Foxn1^{nu}*) were each tested as individual factors. Post hoc significance testing was performed and corrected for multiple comparison by using the Holm–Šidák approach. BAT ^{18}F-FDG uptake (SUV), tumor weights (mg), tumor ^{18}F-FDG uptake (SUV), and adrenal weights (mg) were tested by using 2-way ANOVA; housing and *Prdkc^{scid}* or NU-*Foxn1^{nu}* were tested as individual factors, and posthoc significance testing was performed and corrected for multiple comparisons by using the Holms–Šidák approach. Data sets were tested for homoscedasticity and gross normality to confirm the assumptions of the models were not violated. The α level for all data sets was set to 0.050. All calculations were performed in Stata 12 (version 12.1, StataCorp, College Station, TX). Figures were created in Prism 6 (version 6.01, GraphPad Software, La Jolla, CA) and are presented as routine box-and-whisker plots, with boxes representing the 25th and 75th percentiles and whiskers representing the minimal and maximal data points.

Results

Effect of housing on BAT activation. Statistical analysis of longitudinal thermography measurements of nonshivering thermogenesis (ΔT BAT, °C) revealed that housing has a significant effect on ΔT BAT ($F_{2,87} = 17.89$, $P < 0.001$), accounting for 52% of the total variation, whereas the effect of mouse phenotype was not significant ($F_{1,87} = 2.65$, $P = 0.107$). The interaction between housing and phenotype was significant ($F_{2,87} = 6.06$, $P = 0.003$), accounting for 11% of the total variation. The day-to-day measurements did not vary significantly ($F_{1,138} = 1.04$, $P = 0.309$). *Prdkc^{scid}* mice housed in IVC exhibited greater acute BAT activation compared with those in static cages ($F_{2,87} = 9.92$, $P < 0.001$) or IVC with shelters ($F_{2,87} = 22.63$, $P < 0.001$). *Prdkc^{scid}* mice in static cages exhibited more ($F_{2,87} = 7.87$, $P < 0.001$) acute BAT activation than did those in IVC with shelters. The trend was similar in NU-*Foxn1^{nu}* mice: mice housed in IVC exhibited greater BAT activation than did those in static cages ($F_{2,87} = 13.18$, $P < 0.001$) or IVC with shelters ($F_{2,87} = 17.87$, $P < 0.001$). NU-*Foxn1^{nu}* mice housed in static cages had more BAT activation than did those housed in IVC with shelters ($F_{2,87} = 3.96$, $P = 0.022$; Figure 1 A and B).

On statistical analysis, 70% of the variation in BAT vacuolation was accounted for by housing group ($F_{2,18} = 102.99$, $P < 0.001$) and 7% by mouse phenotype ($F_{1,18} = 21.21$, $P < 0.001$). The interaction was significant ($F_{2,18} = 23.93$, $P < 0.001$), accounting for 16% of the total variation. In *Prdkc^{scid}* mice, BAT histologically had smaller vacuoles in animals housed in IVC compared with static cages ($F_{2,18} = 16.04$, $P < 0.001$) and in mice housed in IVC with shelters ($F_{2,18} = 3.78$, $P = 0.043$). *Prdkc^{scid}* mice housed in IVC with shelters had smaller ($F_{2,18} = 5.26$, $P = 0.016$) vacuoles than did mice housed in static cages (Figure 1 C and D). NU-*Foxn1^{nu}* mice housed in IVC or IVC with shelters had smaller ($F_{2,18} = 18.05$, $P < 0.001$) vacuoles than those housed in statics cages, but there was no significant difference between mice housed in IVC and those in IVC with shelters ($F_{2,18} = 0.42$, $P = 0.662$; Figure 1 C). The histologic analysis demonstrates greater chronic activation of BAT in mice housed in IVC compared with static cages and that 3-wk exposure to shelters partially rescues this effect in *Prdkc^{scid}* but not NU-*Foxn1^{nu}* mice (Figure 1 C).

We quantitatively measured BAT glucose metabolism by injecting mice with the glucose analog ^{18}F-FDG, allowing ^{18}F-FDG uptake to take place in the home cage, and PET scanning the mice. BAT ^{18}F-FDG uptake differed ($F_{2,18} = 3.79$, $P = 0.042$) between the housing conditions, accounting for 26% of the total variance, but posthoc testing revealed no significant difference between any groups (Figure 1 E). Mouse phenotype ($F_{1,18} < 0.01$, $P = 0.935$) and the interaction of phenotype and housing ($F_{2,18} = 0.86$, $P = 442$) did not influence BAT ^{18}F-FDG uptake. During the uptake period, we observed that the mice were very active after injection and that the animals did not return to the shelters for 25 ± 7 min (mean ± 1 SD; *Prdkc^{scid}* mice) or 29 ± 6 min (NU-*Foxn1^{nu}*) after injection, well after the peak uptake time.[10]

Influence of housing type on subcutaneous tumors. The size of subcutaneous tumors size varied by housing type ($F_{2,18} = 33.43$, $P < 0.001$) and mouse phenotype ($F_{1,18} = 22.57$, $P < 0.001$), accounting for 54% and 18% of the total variance, respectively. The interaction of these parameters was significant ($F_{2,18} = 8.46$, $P < 0.001$), accounting for 14% of the total variance. Subcutaneous tumors at 14 d after implantation were smaller in *Prdkc^{scid}* mice housed in IVC compared with static cages ($F_{2,18} = 4.55$, $P = 0.025$) but did not differ from those of mice housed in IVC with shelters ($F_{2,18} = 3.48$, $P = 0.053$; Figure 2 A). Tumors grown in *Prdkc^{scid}* mice housed in IVC with shelters or static cages did not differ ($F_{2,18} = 0.54$, $P = 0.594$). Tumors grown in NU-*Foxn1^{nu}*
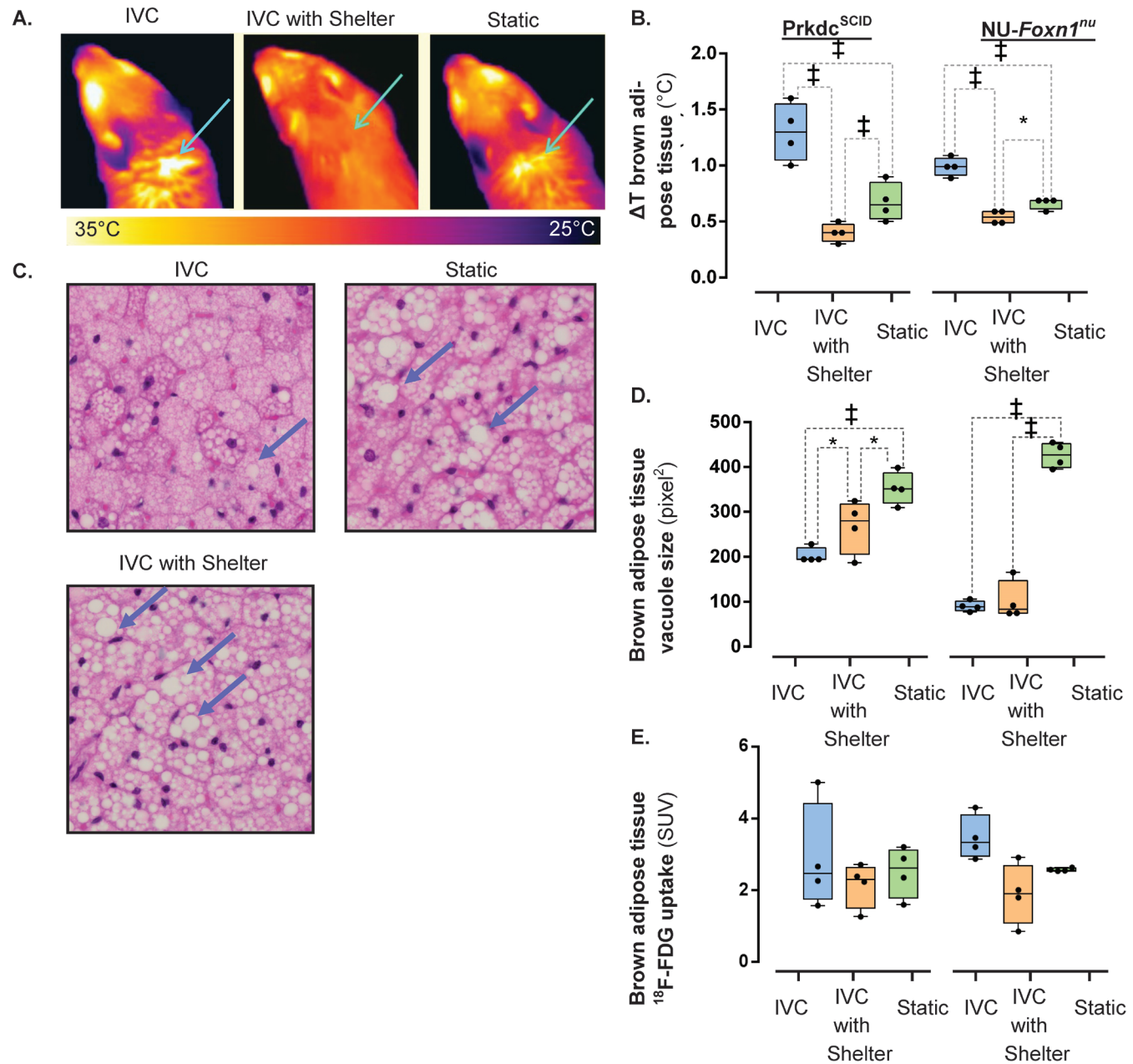
Figure 1. The influence of ventilated caging and shelters on BAT activity. Acute BAT activation is (A) visualized (arrow) and (B) quantified (ΔT BAT, °C) by thermography in Prkdc*scid* and NU-*Foxn1nu* mice (*n* = 4). (C) Vacuoles in BAT (arrow) were (D) significantly smaller in Prkdc*scid* and NU-*Foxn1nu* mice housed in IVC. (E) The effect of housing on ^{18}F-FDG uptake in BAT, as quantified by PET. *, $P < 0.050$; ‡, $P < 0.001$.

mice housed in IVC were smaller than those of mice housed in IVC with shelters ($F_{2,18}$ = 10.62, $P < 0.001$) or static cages ($F_{2,18}$ = 23.34, $P < 0.001$). Subcutaneous tumors grown in NU-*Foxn1nu* mice housed in IVC with shelters were smaller than those of mice housed in static cages ($F_{2,18}$ = 12.47, $P < 0.001$; Figure 2 A). Therefore subcutaneous tumors can grow significantly more slowly in mice housed in IVC compared with static cages. Shelters partially rescued the IVC-associated effects on subcutaneous tumor growth in NU-*Foxn1nu* mice.

Tumor ^{18}F-FDG was effected by housing type ($F_{2,18}$ = 35.50, $P < 0.001$), accounting for 76% of the total variance, while mouse phenotype did not alter tumor ^{18}F-FDG uptake ($F_{1,18}$ = 2.33, $P = 0.144$). The interaction was not significant ($F_{2,18}$ = 0.91, $P = 0.420$).Tumor ^{18}F-FDG uptake in PET scans in *Prdkcscid* mice housed in IVC was significantly lower than that of mice housed

in static cages ($F_{2,18}$ = 18.17, $P < 0.001$) but not IVC with shelters ($F_{2,18}$ = 0.21, $P = 0.814$; Figure 2 B and C). *Prdkcscid* mice housed in IVC with shelters had significantly ($F_{2,18}$ = 8.513, $P = 0.003$) lower uptake in tumors than did those in housed in static cages. ^{18}F-FDG uptake of tumors in NU-*Foxn1nu* mice housed in IVC was lower than that of tumors implanted in mice housed in static cages ($F_{2,18}$ = 9.68, $P = 0.001$) but not IVC with shelters ($F_{2,18}$ = 0.14, $P = 0.869$) (Figure 2 B and C). Tumors in NU-*Foxn1nu* mice housed in IVC with shelters had significantly ($F_{2,18}$ = 7.21, $P = 0.004$) lower ^{18}F-FDG uptake than did mice housed in static cages (Figure 2 B and C). The PET quantification demonstrates that there is a significant difference in tumor glycolytic metabolism between mice housed in IVC compared with static cages.

Adrenal size under various housing conditions. Adrenal size was significantly affected by housing condition ($F_{2,18}$ = 35.50, $P <$

0.001) and mouse phenotype ($F_{1,18} = 9.16$, $P = 0.007$), accounting for 63% and 10% of the total variance, respectively; their interaction was not significant ($F_{2,18} = 3.34$, $P = 0.058$). Adrenal weights were greater in *Prdkc^scid* mice housed in IVC compared with IVC with shelters ($F_{2,18} = 8.95$, $P < 0.001$) or static cages ($F_{2,18} = 23.34$, $P < 0.001$). Adrenal weights of *Prdkc^scid* mice housed in IVC with shelters did not differ from those of mice housed in static cages ($F_{2,18} = 0.19$, $P = 0.831$). The adrenal weight of NU-*Foxn1^nu* mice housed in IVC was greater than that of those housed in static cages ($F_{2,18} = 4.51$, $P = 0.030$) but not IVC with shelters ($F_{2,18} = 3.03$, $P = 0.074$). Adrenal weights in NU-*Foxn1^nu* mice did not differ ($F_{2,18} = 0.19$, $P = 0.831$) between those housed in IVC with shelters compared with static cages (Figure 3).

Discussion

Our data demonstrate that mice experience significantly greater cold stress when housed in housed in IVC compared with static cages. Mice in IVC express have greater acute non-shivering thermogenesis, smaller BAT vacuoles (indicating chronic BAT activation),[25] and larger adrenal glands than do mice housed in static cages. Although neuroendocrine metrics were beyond the scope of the study design, the enlarged adrenal glands we observed are consistent with previously described cold-mediated hypothalamic activation, with subsequent sympathetic cascades associated with nonshivering thermogenesis in β₃-receptor–rich BAT.[20,29] This mechanism is well conserved among mammals and occurs in multiple species, including rodents and humans.[29] However, we did not investigate the mechanism and cannot rule out other explanations, such as psychologic stress associated with IVC. In addition to the physiologic consequences of IVC, subcutaneously tumors were smaller and had less glycolytic metabolism when implanted in both *Prdkc^scid* and NU-*Foxn1^nu* mice housed in IVC compared with static cages. In light of the BAT activation we observed in the current study and previous reports of cold sensitivity in subcutaneous tumors,[10] these data are consistent with the hypothesis that housing-dependent cold stress blunts tumor growth. These findings have implications for investigators in numerous fields, including metabolism, oncology, and endocrinology.

In contrast to other experimental metrics, the ^{18}F-FDG BAT uptake data did not support the hypothesis that mice housed in IVC are cold-stressed more than are mice housed in static cages. We believe this finding is due to the observer effect, an artifact created by experimental manipulation: rodents exhibit a hyperthermic response to handling.[31] We transitionally reduced the cold stress imposed by IVC by handling the animals prior to the experiment and reduced metabolic activity in BAT.

However, the tumor ^{18}F-FDG uptake data did support the hypothesis that IVC decrease tumor metabolism, indicating that housing condition does affect tumor metabolism. However, the data did not support the hypothesis that shelters can rescue the effects of IVC. This finding is best explained by a previous observation that approximately 80% of ^{18}F-FDG uptake after intraperitoneal injection of subcutaneous tumors (glioblastoma, U251) is completed within approximately 30 min.[10] As the animals were very active after injection, most of the ^{18}F-FDG we injected was likely already retained within the tumor by the time the mice returned to their shelters, thereby bypassing any potential rescue effect of the shelters. Despite the technical issues associated with measuring thermo-stress by assessing ^{18}F-FDG uptake in conscious mice, we discovered a very important finding: the growth and basal glycolytic metabolism of subcutaneous tumors varies by housing type. This effect creates
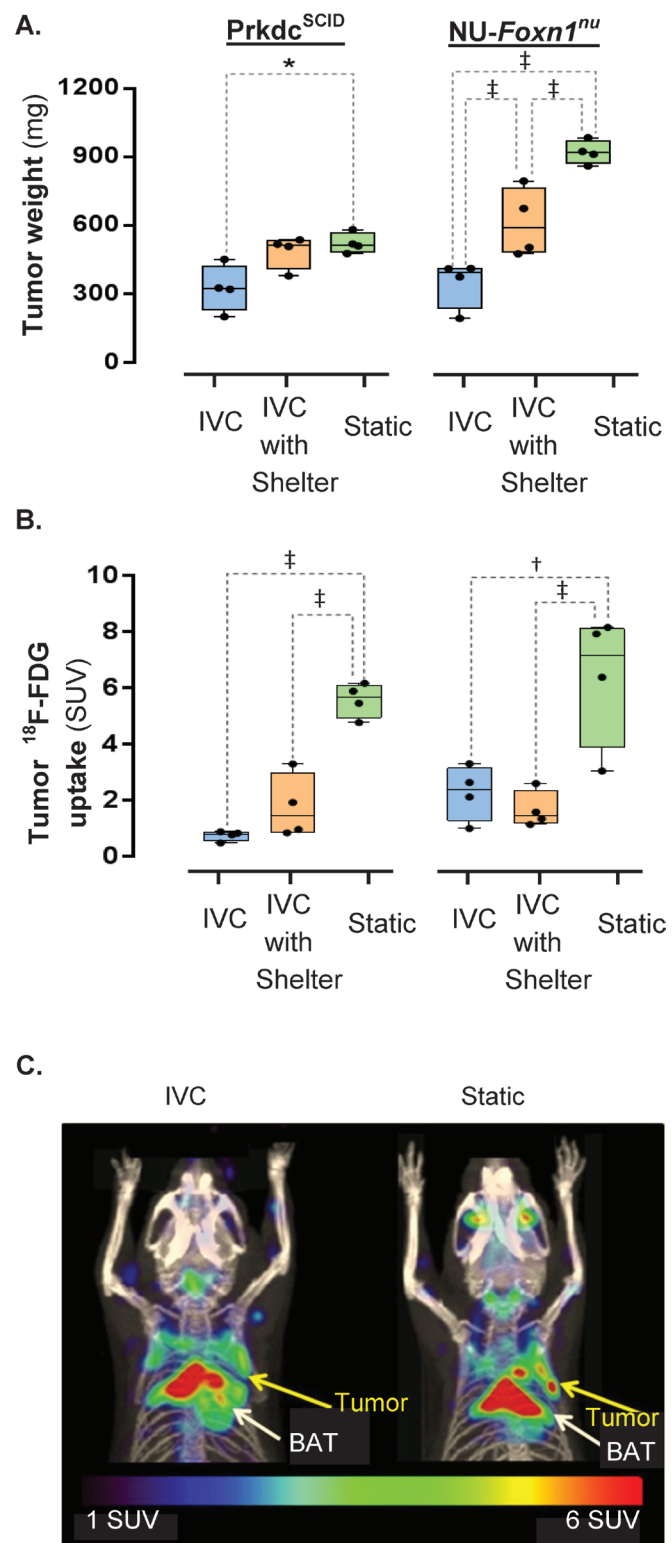

Figure 2. The effect of ventilated caging and shelters on tumor size and metabolism. (A) The size of a subcutaneous epitheloid carcinoma (A431) at 14 d after implantation in *Prdkc^scid* and NU-*Foxn1^nu* mice housed in IVC, IVC with shelters, and static cages. (B) Glycolytic metabolism of subcutaneous epitheloid carcinomas (A431; yellow arrow in panel C) in *Prdkc^scid* and NU-*Foxn1^nu* mice was visualized and quantitated by using (C) fused ^{18}F-FDG PET–CT images (maximal intensity projection, 25-mm slice).*, $P < 0.050$; †, $P < 0.001$; ‡, $P < 0.001$.
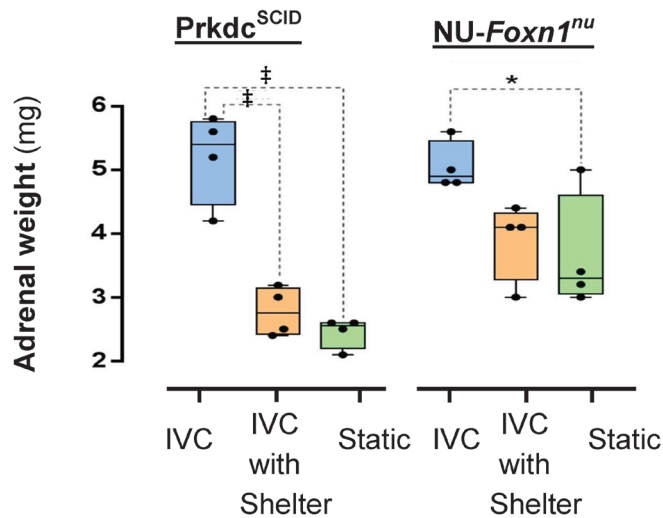
Figure 3. The influence of ventilated caging and shelters on adrenal size. Gross adrenal weights of Prkdc*scid* and NU-*Foxn1nu* mice housed in IVC, IVC with shelters, and static cages. *, $P < 0.050$; ‡, $P < 0.001$.

systematic artifacts in murine models of oncology and may account, in part, for the difficultly of replicating murine research results across institutions,[37] which often vary in husbandry practices. Fortunately, shelters can partially rescue the cold stress imposed by IVC: nonshivering thermogenesis was lower in mice of both strains that were housed in IVC with shelters compared with IVC or static cages; vacuole size was partially recused in *Prdkcscid* mice (but not significantly NU-*Foxn1nu* mice); tumor weights were partially rescued in NU-*Foxn1nu* mice and showed a trend toward rescue in *Prdkcscid* mice; and adrenal enlargement was recused completely in NU-*Foxn1nu* mice and partially in *Prdkcscid* mice. We speculate that the mechanism of shelter-associated rescue of cold stress in our study reflects the combined effects of an area free of air flow and the increased retention of radiated heat in a 3D shelter.

These results highlight the importance that behaviorally maintained heated microclimates play in the homeostasis of murine physiology and, in turn, experimental results. Our data demonstrate that allowing mice to behaviorally thermoregulate in IVC reduces physiology stress and benefits scientists by improving uniformity in physiologic states and experimental results across housing systems (at least, in the context of ubiquitous subcutaneous tumor models). In addition, this work in combination with a previous observation that mice prefer to minimize energy expenditures[18] supports the notion that shelters are a great refinement to IVC housing. However, we cannot distinguish the motivation driving the observed thermoregulatory behavior: the motivation could be seeking heat (thermotaxis), seeking enclosed space (thigmotaxic), or some other factor. Nonetheless, the physiologic benefits of accommodating enhanced behavioral thermoregulation are consistent with previous behavioral findings that nesting material blunts aversion to IVC.[1]

Placing mice in barren cages limits their behavior, the preferred and primary murine thermoregulatory tool.[12,13,17,18] To minimize variables in laboratory mice yet capitalize on the benefits of IVC, the laboratory animal community should strive to reduce and standardize the cold-stress experience of mice housed under our care. Potential approaches to this issue include raising the macroenvironmental temperature, adding large amounts (for example, 10 g) of nesting material,[12] adding rigid shelters (like the one used in this study), engineering modi-

fications to IVC and ventilated racks to minimize cold stress, and using Illinois cabinets to better control microenvironments (for example, conditioned air).

Each approach has disadvantages: raising macroenvironmental temperatures may lead to heat exhaustion due to the narrow and strain-dependent thermoneutral zones of mice (which span 1 to 3 °C),[17] increase energy costs, and may cause discomfort in husbandry staff. Although elevations in ambient temperatures have been suggested to increase aggression among cagemates,[11] the effect is limited to introducing novel males and is transient, mostly dissipating over the first hour after introduction.[19] Nesting material has been shown to blunt heat-seeking behavior in mice[11] but has the disadvantage of obstructing visualization of the animals, making daily monitoring cumbersome when applied to a large-scale facility. The translucent, red shelters that we used in the current study are an appealing middle ground, maintaining murine homeostasis while providing animal visibility. However, wheel-mount shelters increase male–male aggression in mice,[22] hinting at a possible welfare concern associated with rigid shelters. Moreover, we demonstrated a significant (but incomplete) physiologic rescue with shelters, limiting their usefulness as a sole solution. Engineering changes to IVC, ventilated racks, or Illinois cabinets require time, research, and capital investment in new systems.

These issues are complex, and few comparison studies are available. The few studies to date use different metrics and strains, which are known to vary in cold sensitivity,[17] thereby complicating comparisons.[16] In light of the difficulty comparing environmental enrichment studies,[36] we highlight the specifics of this study that may limit its comparison with other work on enrichment. Both Prdkc*scid* and Nu-*Foxn1Nu* mice, selected for their ability to propagate human tumors, are deficient in lymphocyte populations. Although not described in the literature to play a role in thermoregulatory functions, our findings could be phenotype-specific. Phenotype-associated variations are especially pertinent to the hairless NU-*Foxn1nu* mice we used study, which are known to be particularly cold-prone.[6] In addition, we removed the cofounder of social huddling, which has thermoregulatory benefits,[21] by singly housing the mice. The corncob bedding, routine in our vivarium, likely provides less insulation than do more malleable substrates. Therefore, mice housed in large social groups or on more highly insulating bedding may be less cold-stressed in IVC than were the mice in our study. Finally, this study used male mice. Housing consequences can be sex-specific: for example, IVC induced greater anxiety in female mice.[27] Additional studies are required to illuminate these intricacies.

A balanced, hybrid solution—such as combining engineering modifications with slightly higher macroenvironmental temperatures (for example, by increasing routine housing temperatures to 24 °C) and enriching IVC with nesting material or translucent shelters—likely will minimize the disadvantages of each approach. Additional research is needed to optimize performance standards to promote animal welfare and uniform murine physiology within and between intuitions. Given the pervasiveness of the issue, variability in murine housing, and implications on experimental results, we recommend reporting the housing system and nesting materials used in rodent-dependent research.

References

1. **Baumans V, Schlingmann F, Vonck M, van Lith HA**. 2002. Individually ventilated cages: beneficial for mice and men? Contemp Top Lab Anim Sci **41:**13–19.
2. **Cannon B, Nedergaard J.** 2004. Brown adipose tissue: function and physiological significance. Physiol Rev **84:**277–359.
3. **Cannon B, Nedergaard J.** 2011. Nonshivering thermogenesis and its adequate measurement in metabolic studies. J Exp Biol **214:**242–253.
4. **Celi FS.** 2009. Brown adipose tissue–when it pays to be inefficient. N Engl J Med **360:**1553–1556.
5. **Compton SR, Homberger FR, MacArthur Clark J.** 2004. Microbiological monitoring in individually ventilated cage systems. Lab Anim (NY) **33:**36–41.
6. **David JM, Chatziioannou AF, Taschereau R, Wang H, Stout DB.** 2013. The hidden cost of housing practices: using noninvasive imaging to quantify the metabolic demands of chronic cold stress of laboratory mice. Comp Med **63:**386–391.
7. **Enerback S, Jacobsson A, Simpson EM, Guerra C, Yamashita H, Harper ME, Kozak LP.** 1997. Mice lacking mitochondrial uncoupling protein are cold-sensitive but not obese. Nature **387:**90–94.
8. **Foster DO**. 1984. Quantitative contribution of brown adipose tissue thermogenesis to overall metabolism. Can J Biochem Cell Biol **62:**618–622.
9. **Foster DO, Frydman ML.** 1979. Tissue distribution of cold-induced thermogenesis in conscious warm- or cold-acclimated rats reevaluated from changes in tissue blood flow: the dominant role of brown adipose tissue in the replacement of shivering by nonshivering thermogenesis. Can J Physiol Pharmacol **57:**257–270.
10. **Fueger BJ, Czernin J, Hildebrandt I, Tran C, Halpern BS, Stout D, Phelps ME, Weber WA.** 2006. Impact of animal handling on the results of 18F-FDG PET studies in mice. J Nucl Med **47:**999–1006.
11. **Gaskill BN, Gordon CJ, Pajor EA, Lucas JR, Davis JK, Garner JP.** 2012. Heat or insulation: behavioral titration of mouse preference for warmth or access to a nest. PLoS ONE **7:**e32799.
12. **Gaskill BN, Gordon CJ, Pajor EA, Lucas JR, Davis JK, Garner JP**. 2013. Impact of nesting material on mouse body temperature and physiology. Physiol Behav **110–111:**87–95.
13. **Gaskill BN, Rohr SA, Pajor EA, Lucas JR, Garner JP.** 2009. Some like it hot: mouse temperature preferences in laboratory housing. Appl Anim Behav Sci 116**:**279–285.
14. **Geiger R, Aron RH, Todhunter P**. 2009. The climate: near the ground. Lanham (MA): Rowman and Littelfield Publishers.
15. **Giard DJ, Aaronson SA, Todaro GJ, Arnstein P, Kersey JH, Dosik H, Parks WP.** 1973. In vitro cultivation of human tumors: establishment of cell lines derived from a series of solid tumors. J Natl Cancer Inst **51:**1417–1423.
16. **Gonder JC, Laber K.** 2007. A renewed look at laboratory rodent housing and management. ILAR J **48:**29–36.
17. **Gordon C.** 2012. Thermal physiology of laboratory mice: defining thermoneutrality. J Therm Biol **37:**654–685.
18. **Gordon CJ.** 1985. Relationship between autonomic and behavioral thermoregulation in the mouse. Physiol Behav **34:**687–690.
19. **Greenberg G.** 1972. The effects of ambient temperature and population density on aggression in two inbred strains of mice, *Mus musculus*. Behaviour **42:**119–130.
20. **Harvey PW, Sutcliffe C.** 2010. Adrenocortical hypertrophy: establishing cause and toxicological significance. J Appl Toxicol **30:**617–626.
21. **Heldmaier G**. 1975. The influence of the social thermoregulation on the cold-adaptive growth of BAT in hairless and furred mice. Pflugers Archiv **355:**261–266.
22. **Howerton CL, Garner JP, Mench JA.** 2008. Effects of a running wheel-igloo enrichment on aggression, hierarchy linearity, and stereotypy in group-housed male CD-1 (ICR). Appl Anim Behav Sci **115:**90–103.
23. **Kostomitsopoulos NG, Paronis E, Alexakos P, Balafas E, van Loo P, Baumans V.** 2007. The influence of the location of a nest box in an individually ventilated cage on the preference of mice to use it. J Appl Anim Welf Sci **10:**111–121.
24. **Lange K, Carson R.** 1984. EM reconstruction algorithms for emission and transmission tomography. J Comput Assist Tomogr **8:**306–316.
25. **Lim S, Honek J, Xue Y, Seki T, Cao Z, Andersson P, Yang X, Hosaka K, Cao Y.** 2012. Cold-induced activation of brown adipose tissue and adipose angiogenesis in mice. Nat Protoc **7:**606–615.
26. **Lodhi IJ, Semenkovich CF.** 2009. Why we should put clothes on mice. Cell Metab **9:**111–112.
27. **Logge W, Kingham J, Karl T.** 2013. Behavioural consequences of IVC cages on male and female C57BL/6J mice. Neuroscience **237:**285–293.
28. **Ma S, Yu H, Zhao Z, Luo Z, Chen J, Ni Y, Jin R, Ma L, Wang P, Zhu Z, Li L, Zhong J, Liu D, Nilius B.** 2012. Activation of the cold-sensing TRPM8 channel triggers UCP1-dependent thermogenesis and prevents obesity. J Mol Cell Biol **4:**88–96.
29. **Morrison SF, Nakamura K, Madden CJ.** 2008. Central control of thermogenesis in mammals. Exp Physiol **93:**773–797.
30. **Nguyen KD, Qiu Y, Cui X, Goh YP, Mwangi J, David T, Mukundan L, Brombacher F, Locksley RM, Chawla A.** 2011. Alternatively activated macrophages produce catecholamines to sustain adaptive thermogenesis. Nature **480:**104–108.
31. **Romanovsky AA, Kulchitsky VA, Simons CT, Sugimoto N.** 1998. Methodology of fever research: why are polyphasic fevers often thought to be biphasic? Am J Physiol **275:**R332–R338.
32. **Rudaya AY, Steiner AA, Robbins JR, Dragic AS, Romanovsky AA.** 2005. Thermoregulatory responses to lipopolysaccharide in the mouse: dependence on the dose and ambient temperature. Am J Physiol Regul Integr Comp Physiol **289:**R1244–R1252.
33. **Seale P, Bjork B, Yang W, Kajimura S, Chin S, Kuang S, Scime A, Devarakonda S, Conroe HM, Erdjument-Bromage H, Tempst P, Rudnicki MA, Beier DR, Spiegelman BM.** 2008. PRDM16 controls a brown fat/skeletal muscle switch. Nature **454:**961–967.
34. **Suckow MA, Stevens KA, Wilson RP.** 2012. The laboratory rabbit, guinea pig, hamster, and other rodents. Waltham (MA): Academic Press/Elsevier.
35. **Swoap SJ, Overton JM, Garber G.** 2004. Effect of ambient temperature on cardiovascular parameters in rats and mice: a comparative approach. Am J Physiol Regul Integr Comp Physiol **287:**R391–R396.
36. **Toth LA, Kregel K, Leon L, Musch TI.** 2011. Environmental enrichment of laboratory rodents: the answer depends on the question. Comp Med **61:**314–321.
37. Troublesome variability in mouse studies. 2009. Nat Neurosci **12:**1075.
38. **van der Veen DR, Shao J, Chapman S, Leevy WM, Duffield GE.** 2012. A diurnal rhythm in glucose uptake in brown adipose tissue revealed by in vivo PET-FDG imaging. Obesity (Silver Spring) **20:**1527–1529.
39. **Wang H, Stout DB, Chatziioannou AF**. 2012. Mouse atlas registration with non-tomographic imaging modalities-a pilot study based on simulation. Mol Imaging Biol **14:**408–419.
40. **Wang H, Stout DB, Taschereau R, Gu Z, Vu NT, Prout DL, Chatziioannou AF.** 2012. MARS: a mouse atlas registration system based on a planar x-ray projector and an optical camera. Phys Med Biol **57:**6063–6077.